Ion Pairing and Solvent Relaxation Processes in Aqueous Solutions of Sodium Malonate and Sodium Succinate

Andrew Tromans, Peter M. May, and Glenn Hefter*
Chemistry Department, Murdoch University, Murdoch, WA 6150, Australia

Takaaki Sato† and Richard Buchner*
Institut für Physikalische und Theoretische Chemie, Universität Regensburg, D-93040 Regensburg, Germany
Received: April 1, 2004; In Final Form: July 1, 2004

Dielectric relaxation spectra have been measured for aqueous solutions of sodium malonate and sodium succinate over a wide range of frequencies ($0.2 \leq \nu/\text{GHz} \leq 89$) and solute concentrations ($0.025 \leq c/\text{M} \leq 1.0$). In addition to the usual processes associated with bulk water, two further relaxation processes were detected. The faster of these, with a relaxation time of ~16 ps, is unusual and was attributed to the presence of "slow" water in the hydration shells of the anions. The extent of this hydration shell is rather "fragile" (concentration-dependent) for malonate but not for succinate. The second, slower, process was attributed to the presence of ion pairs NaX^-(aq). Unambiguous determination of the structure of the ion pair was not possible because of the internal flexibility of the anions, but the data were most consistent with a chelated solvent-shared ion pair. The kinetics of formation and dissociation of the ion pairs were evaluated from the effects of solute concentration on their relaxation times.

1. Introduction

Sodium malonate (Na_2Ma) and sodium succinate (Na_2Su) are important low-molecular-weight dicarboxylate salts that are found in various environmental, biological, and industrial situations. For example, succinate occurs in photochemical smogs[1] and human blood plasma[2] and is an important component of the citric acid cycle,[3] whereas malonate is known to inhibit tissue respiration.[3] Both species form during the extraction of alumina via the Bayer process, as a result of the decomposition of humic impurities present in typical bauxitic ores.[4] Because of their simple structures, such salts serve as useful models for understanding the behavior of more complex organic species.[5]

Although the common physicochemical properties of sodium malonate and sodium succinate solutions have been studied,[6,7] little is known about their level of ion pairing or the state of hydration of their component ions. Recently, we have shown that dielectric relaxation spectroscopy (DRS), which probes the interaction of a sample with an applied electric field $\vec{E}(\nu)$ at microwave frequencies, provides valuable insights into the nature of aqueous solutions of sodium oxalate (Na_2Ox).[8] In that study, despite the limited solubility of the salt, DRS was able to quantitatively characterize both the thermodynamics and the kinetics of the weak ion association between Na^+(aq) and Ox^{2-}(aq) and to identify the structure of the complex formed as a double-solvent-separated ion pair (2SIP). In addition, useful estimates of the state of hydration of the free ions could be made, and it was shown that the hydration sheath of Ox^{2-}(aq), although extensive, was unusually "fragile", in that it decreased markedly with concentration.

These findings have implications in numerous areas including modeling of the physicochemical properties of Bayer process solutions, simulation of chemical speciation in human blood plasma, and understanding of the behavior of biological macromolecules containing the carboxylate moiety.[9] It was therefore thought worthwhile to extend the previous DRS measurements on Na_2Ox(aq) to sodium malonate and sodium succinate, the next two congeners in the series of straight-chain saturated dicarboxylates.

2. Experimental Section

Sodium malonate monohydrate ($Na_2C_3H_2O_4 \cdot H_2O$) and sodium succinate hexahydrate ($Na_2C_4H_3O_4 \cdot 6H_2O$), with stated purities of ≥99%, were used as received from Sigma-Aldrich, St. Louis, MO. Solutions were prepared volumetrically, without buoyancy corrections, using high-purity water (Millipore Milli-Q systems) and A-grade volumetric glassware. Solution concentrations were determined to ±0.2% relative by back-titration against sodium hydroxide [BDH Chemicals Ltd., Poole, U.K., concentrated volumetric standard (CVS)] after addition of excess HCl (BDH Chemicals Ltd., CVS). Densities were determined using a vibrating-tube density meter (Anton Paar GmbH, Graz, Austria, model DMA 602, connected to an mPDS 4000 evaluation unit). Solution temperatures were controlled to 25 ± 0.01 °C with an accuracy of ±0.02 °C with a Julabo (Seelbach, Germany, model F-33) refrigerated thermostat-circulator.

Low-frequency data ($\nu_{\min} \leq \nu/\text{GHz} \leq 20$) were measured at Murdoch University using a Hewlett-Packard model 85070 M dielectric probe system based on an HP 8720D vector network analyzer (VNA). The system temperature was controlled with a Hetofrig (Heto, Denmark) thermostat−circulator to 25 ± 0.02 °C and an accuracy of ~0.05 °C. The VNA was calibrated at the target temperature using air, mercury, and water as standards. Calibration parameters for water were obtained from the literature.[10] All spectra were measured at least twice using separate calibrations. Measurements were made at a total of 101 frequencies between $\nu_{\min}$ and 20 GHz, equally spaced on a logarithmic scale. The value of $\nu_{\min}$ was determined by the

* To whom correspondence should be addressed. Email: hefter@chem.murdoch.edu.au (G.H.), Richard.Buchner@chemie.uni-regensburg.de (R.B.).
† Permanent address: Department of Applied Physics, School of Science and Engineering, Waseda University, Okubo, Shinjuku-ku, Tokyo 169-8555, Japan.

10.1021/jp048575w CCC: $27.50
Published on Web 08/14/2004

conductivity of the sample solution but was typically in the range $0.2 \leq \nu_{min}/\text{GHz} \leq 0.4$. High-frequency data were measured at Regensburg using two interferometers: A-band ($27 \leq \nu/\text{GHz} \leq 39$) and E-band ($60 \leq \nu/\text{GHz} \leq 89$) at selected frequencies using procedures described in detail elsewhere.[11,12] Temperature control was obtained by a system similar to that used at Murdoch and was of similar accuracy.

Refractive indices at the sodium D line, n_D^{25}, of the salt solutions were determined at 25 ± 0.05 °C with an Abbé refractometer (Atago, Tokyo, Japan) calibrated with aqueous sucrose solutions.

3. Data Analysis

DRS measures the complex dielectric permittivity

$$\hat{\epsilon}(\nu) = \epsilon'(\nu) - i\epsilon''(\nu) \quad (1)$$

of a sample as a function of the frequency ν of an applied electromagnetic field [$i^2 = -1$]. The in-phase component, $\epsilon'(\nu)$, is the relative dielectric permittivity, while $\epsilon''(\nu)$, the out-of-phase component, represents the dielectric loss. For an electrolyte solution, only the total loss

$$\eta''(\nu) = \epsilon''(\nu) + \kappa/(2\pi\nu\epsilon_0) \quad (2)$$

is measurable, where $\kappa/(2\pi\nu\epsilon_0)$ represents the conductivity contribution from the electrolyte and ϵ_0 is the permittivity of free space. The conductivity term, which dominates at low frequencies and at high electrolyte concentrations, can be evaluated by separate measurement or, as shown previously, by careful fitting of the dielectric data.[10]

The recorded spectra were analyzed by simultaneous fitting of both in-phase and out-of-phase components to relaxation models of the type

$$\hat{\epsilon}(\nu) = \sum_{j=1}^{n} \frac{\epsilon_j - \epsilon_{j+1}}{[1 + (i2\pi\tau_j)^{1-\alpha_j}]^{\beta_j}} + \epsilon_\infty \quad (3)$$

In principle, the high-frequency permittivity, ϵ_∞, measures only the intramolecular polarizability contribution and is used as an adjustable parameter, together with the relative permittivities, ϵ_j, and dielectric relaxation times, τ_j, of the jth process and their attendant relaxation-time distribution parameters, $0 \leq \alpha_j < 1$ and $0 < \beta_j \leq 1$. The observed static permittivity of a given solution is $\epsilon\ (= \epsilon_1) = \epsilon_\infty + \Sigma S_j$, with $S_j = \epsilon_j - \epsilon_{j+1}$ being the amplitude (relaxation strength) of process j and $\epsilon_\infty = \epsilon_{n+1}$, where n is the total number of distinguishable relaxation processes. In the data evaluation, all reasonable relaxation models with $1 \leq n \leq 5$ were tested using Debye ($\alpha_j = 0, \beta_j = 1$), Cole−Cole ($\beta_j = 1$), and/or Havriliak−Negami functions for the band shapes of the processes j.

For both salts, it was found that, for spectra over the range $\nu_{min} \leq \nu/\text{GHz} \leq 89$, a sum of four Debye equations gave the smallest value of the reduced error function, χ_r^2. Only this 4D model (with $n = 4$ and $\alpha_j = 0$ and $\beta_j = 1$ for $j = 1, ..., 4$) yielded a self-consistent set of relaxation parameters that could be assigned to plausible microscopic processes. Those spectra for which only VNA data were recorded at $\nu \leq 20$ GHz did not cover the high-frequency side of the water relaxation. Accordingly, the fourth (fastest) process did not need to be included, and the major relaxation time of bulk water, $\tau_3(c)$, was fixed at values interpolated from the 4D model. The other relaxation parameters so obtained fitted smoothly into the predictions of the 4D model.

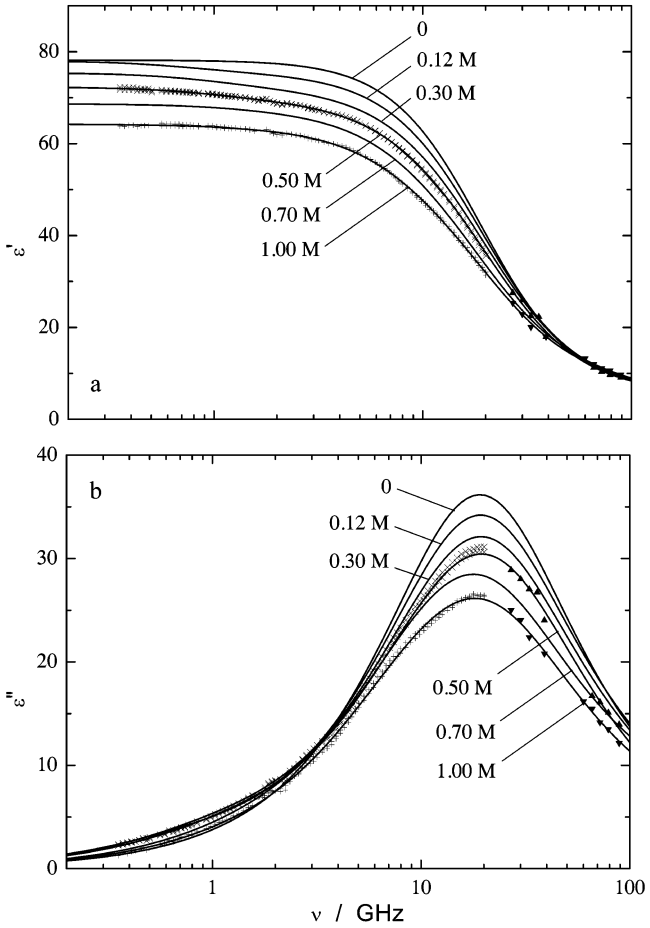

Figure 1. Typical combined DR spectra for $Na_2Ma(aq)$ at 25 °C: (a) dielectric permittivity, $\epsilon'(\nu)$; (b) dielectric loss, $\epsilon''(\nu)$. Data obtained by (+, ×) VNA, (▲, ▼) waveguide interferometers. Solid lines are calculated assuming four Debye processes.

Polarizabilities, α, of Na_2Ma and Na_2Su in aqueous solution, required for use with the Cavell equation (see below), were obtained as described by Born[13] using the molar refraction

$$[R] = \frac{(1-x)M(H_2O) + xM(Na_2Ox)}{\rho} \times \frac{(n_D^{25})^2 - 1}{(n_D^{25})^2 + 2} \quad (4)$$

where x is the mole fraction of the electrolyte in solution and M is its molar mass. The polarizabilities of the anions were obtained by additivity from the salt values by assuming $\alpha(Na^+)/4\pi\epsilon_o = 0.149 \times 10^{-30}\ m^{-3}$, taken from Pyper et al.[14]

4. Results and Discussion

4.1. General Features of the Spectra. Typical permittivity and loss spectra obtained by combining the VNA and interferometric data over the frequency range $\nu_{min} \leq \nu/\text{GHz} \leq 89$ are presented for selected concentrations of Na_2Ma in Figure 1 and Na_2Su in Figure 2. Clearly, there is a virtually seamless fit between the data obtained by the two instruments at all concentrations. The two sets of VNA data included for 1.00 M Na_2Su illustrate the reproducibility, and the spectra at 0.70 M show the agreement between the VNA results and an overlapping set of interferometric data (Figure 2). The relaxation parameters obtained by fitting the data for Na_2Ma and Na_2Su to 4D models are summarized in Table 1, along with related statistical information.

Typical contributions of the four Debye processes to a loss spectrum are illustrated for a 0.70 M Na_2Su solution in Figure 3; similar results were obtained for Na_2Ma solutions. The

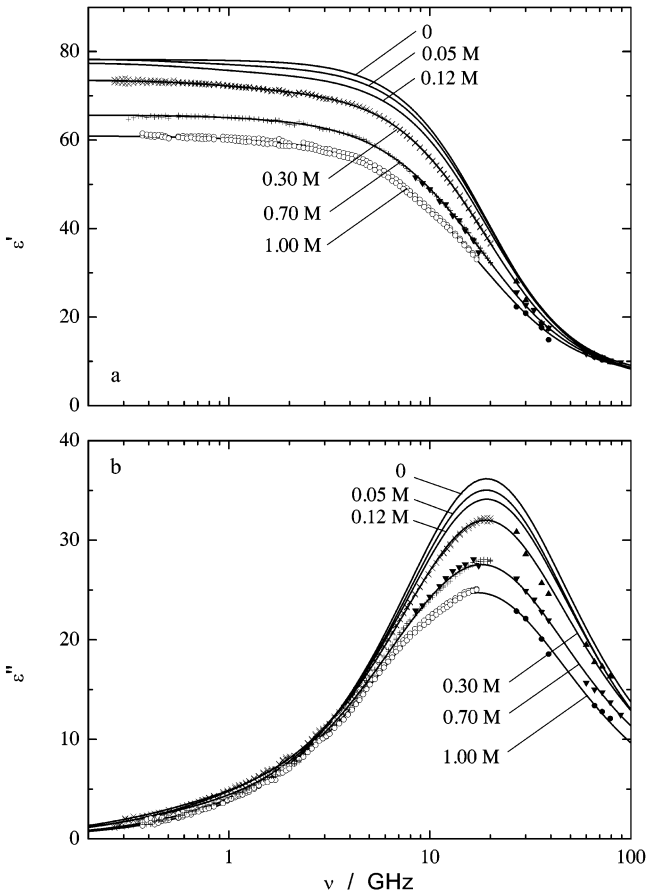

Figure 2. Typical combined DR spectra for Na_2Su(aq) at 25 °C: (a) dielectric permittivity, $\epsilon'(\nu)$; (b) dielectric loss, $\epsilon''(\nu)$. Data obtained by (+, ×, ○) VNA, (▲, ▼, ●) waveguide interferometers. Solid lines are calculated assuming four Debye processes.

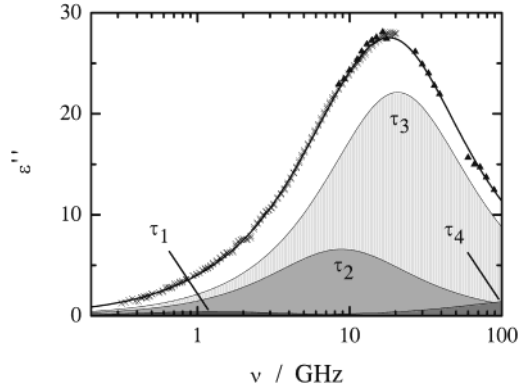

Figure 3. Dielectric loss spectrum $\epsilon''(\nu)$ of 0.700 M Na_2Su(aq) at 25 °C, showing the contributions from the various Debye processes. The solid line is the sum of the four processes.

observed processes include two associated with bulk water: the dominant process centered at ~8 ps (~20 GHz) associated with the cooperative relaxation of the H-bond network and a minor high-frequency process due to the reorientation of mobile water molecules,[10,15] which is barely detectable in the present spectra as a small shoulder at ~90 GHz. In addition, there are two solute-related processes. The slower of these, centered at ~1 GHz and of very small magnitude, is readily assigned to the presence of ion pairs. The faster process, here labeled process 2 (Figure 3), with a relaxation time of ~16 ps (at ~10 GHz), is unusual and is discussed in detail below. It is of sizable amplitude, accounting for about 20−25% of the total water in the solutions of both salts at $c = 1$ M.

4.2. Ion Hydration. The amplitude of process 2 (at ca. 10 GHz) increases markedly with solute concentration, c, but its relaxation time varies only slightly. This is illustrated in Figures 4 and 5 for Na_2Su(aq), with again very similar results being obtained for Na_2Ma(aq). The short relaxation time (~16 ps) of process 2 makes it unlikely, but not impossible, that this process is ion-pair-related (e.g., associated with an internal rotation). However, this would then mean that all water, apart from the relatively minor amounts that might be associated with the ion pairs, must appear in processes 3 and 4. This assumption produces unreasonably large effective solvation numbers (see below): $Z_{ib}(0) \approx 44$ and 23 for Na_2Ma and Na_2Su, respectively. Because $Z_{ib}(0) \approx 4.5$ for Na^+(aq), this implies unrealistically high Z_{ib} values for both Ma^{2-}(aq) and Su^{2-}(aq).[16,8]

Accordingly, it seems more reasonable to assign process 2 to "slow" water associated with Ma^{2-} and Su^{2-} [note that the "irrotationally bound" water associated with Na^+(aq) evidences itself only as an apparent loss of bulk water]. The relaxation times of these slow water molecules are lowered by a factor of ~2 compared with bulk water (~16 vs ~8 ps) but are not sufficiently tightly held to become irrotationally bound as occurs for the oxalate anion. The existence of a process ascribable to slow water is unusual but not unknown: similar processes have been reported in aqueous solutions containing R_4N^+ salts[17] and in various micellar dispersions including $NaROSO_3$(aq), where R = n-$C_{12}H_{25}$.[18,19]

From the amplitudes of the solvent dispersion steps S_2 and $(S_3 + S_4)$, the concentration of slow water, c_2, and the apparent bulk water concentration, c_s^{ap}, were calculated with the solvent-normalized Cavell equation following the procedures outlined in detail elsewhere.[17,20,21] From the comparison of c_s^{ap} with the analytical water concentration, c_s, corrected for c_2 and assuming slip boundary conditions for kinetic depolarization, an effective hydration number at infinite dilution of $Z_{ib}(0) \approx (10 \pm 1.5)$ was obtained (Figure 6) for both Na_2Ma(aq) and Na_2Su(aq). This is about the same as the number of irrotationally bound water molecules that would be expected to be associated with 2 × Na^+(aq).[10] In other words, $Z_{ib}(0) \approx 0$ for both Ma^{2-}(aq) and Su^{2-}(aq), which is in marked contrast to the value of $Z_{ib}(0) \approx 6$ calculated for Ox^{2-}(aq) and the hydration number of 4 obtained for the acetate ion from neutron and X-ray diffraction data.[16]

For Na_2Ox(aq), it was found[8] that Z_{ib} decreased linearly with c, which was shown to be due entirely to the decrease in solvation of Ox^{2-}(aq). Superficially, there also appears to be an appreciable decrease in Z_{ib} for both Na_2Ma(aq) and Na_2Su(aq) with c (the dashed lines in Figure 6). However, as is apparent from the scatter in the data, the uncertainties in Z_{ib} are rather large, mostly because of the difficulties in separating processes 2 and 3, which are broad and overlapping (Figure 3). For example, if the selected values of ϵ_3 for Na_2Su(aq) were altered by 0.5, which is well within the likely experimental errors, Z_{ib} would be independent of c (dotted line in Figure 6b), with an average value of 9 ± 1.5, which is consistent with 2 × $Z_{ib}(Na^+(aq))$.[10,20] Similar results were obtained for Na_2Ma(aq).

The amplitude of process 2, S_2, and thus the concentration of slow water (c_2) for Na_2Su(aq), increases approximately linearly with c (Figure 7b), which signifies a constant number (12.9 ± 0.3) of slow water molecules associated with Su^{2-}(aq). In contrast, for Na_2Ma(aq), there is a parabolic increase in S_2 and c_2 (Figure 7a) consistent with there being about 20 slow water molecules surrounding Ma^{2-}(aq) at infinite dilution, decreasing to ~10 at $c = 1$ M. This decrease in the number of slow water molecules around Ma^{2-}(aq), but not around Su^{2-}(aq),

TABLE 1: Conductivities, κ; Limiting Permittivities, ϵ_j; Relaxation Times, τ_j; and Reduced Error Function Values, χ_r^2, for $Na_2Ma(aq)$ and $Na_2Su(aq)$ at 25 °C[a,b]

c	κ	ϵ_1	τ_1	ϵ_2	τ_2	ϵ_3	τ_3	ϵ_4	τ_4	ϵ_∞	χ_r^2
					$Na_2Ma(aq)$						
0	0					78.32	8.33	6.32	1.1	4.57	
0.0250	0.454	78.66	409			77.82	8.24F	5.51			0.028
0.0500	0.816	78.44	217			77.38	8.17F	4.70			0.028
0.0800	1.19	78.54	206	76.34	15.5	72.17	8.08F	6.47			0.044
0.1200	1.68	78.05	202	75.19	15.5	70.73	8.04	7.00	1F	3.77	0.027
0.1500	2.04	77.86	171	74.70	15.1	70.27	7.99F	6.42			0.056
0.2501	3.11	76.11	153	72.86	15.3	64.88	7.92F	7.29			0.044
0.3000	3.57	75.43	150	71.82	15.1	62.72	7.66	7.09	1F	4.13	0.05
0.3000	3.51	75.26	142	71.94	13.7	61.46	7.70F	6.14			0.113
0.4001	4.42	73.24	134	70.36	16.7	60.65	7.62F	6.95			0.063
0.5001	5.16	72.34	152	69.28	15.6	56.54	7.35	6.30	1F	4.75	0.058
0.6000	5.88	69.78	113	67.74	17.3	55.94	7.52F	7.44			0.042
0.7019	6.43	68.65	107	66.86	16.5	52.62	7.88	8.99	1F	2.37	0.045
0.8011	6.97	67.30	129	65.59	18.7	53.32	7.48F	6.50			0.033
1.0002	7.87	64.24	122	63.25	18.0	48.18	7.44	8.31	1F	4.15	0.061
					$Na_2Su(aq)$						
0.0251	0.413	78.32	304			77.58	8.31F	5.97			0.005
0.0500	0.791	78.42	224	76.77	18.0	75.99	8.28F	6.63			0.033
0.0800	1.18	78.07	223	75.93	21.7	75.13	8.26F	6.51			0.027
0.1206	1.66	77.50	198	74.90	17.5	73.16	8.25	7.04	1F	4.68	0.048
0.1601	2.04	76.56	182	74.11	17.5	71.77	8.18F	6.04			0.022
0.2001	2.49	76.01	169	73.20	18.7	71.18	8.15F	6.46			0.022
0.2501	2.92	74.63	185	72.04	18.2	67.62	8.10F	6.51			0.044
0.3000	3.45	73.57	149	71.15	17.2	65.39	8.06	6.75	1F	4.13	0.064
0.4000	4.25	71.55	156	69.52	18.4	62.40	7.97F	6.54			0.031
0.5142	5.17	69.59	160	67.39	17.7	58.64	7.81	6.84	1F	6.14	0.053
0.7000	6.13	65.66	131	64.81	18.0	51.64	7.70	7.37	1F	4.25	0.062
1.0000	7.27	60.95	156	60.15	18.2	43.96	7.44	7.18	1F	5.63	0.113

[a] Parameter values followed by the letter F were not adjusted in the fitting procedure. Data for pure water were taken from ref 15. [b] Units: c in M, κ in $\Omega^{-1}\cdot m^{-1}$, τ_j in 10^{-12} s.

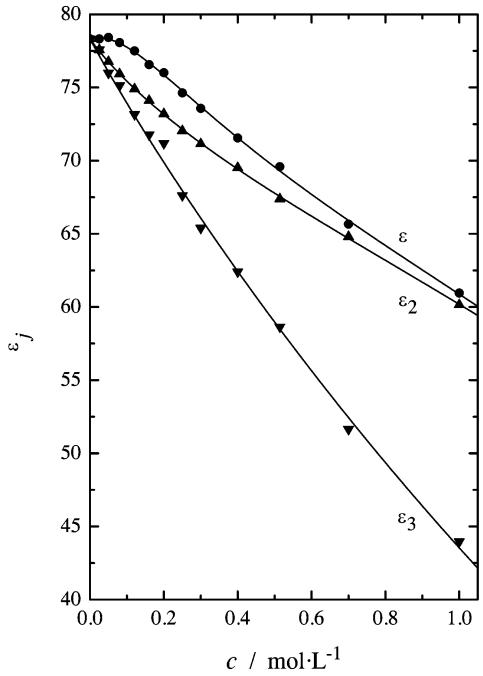

Figure 4. Measured limiting permittivities ϵ_j ($j = 1, 2, 3$) for $Na_2Su(aq)$ at 25 °C as a function of solute concentration, where $\epsilon = \epsilon_1$ refers to the ion-pair process, ϵ_2 the slow water relaxation, and ϵ_3 the bulk water relaxation.

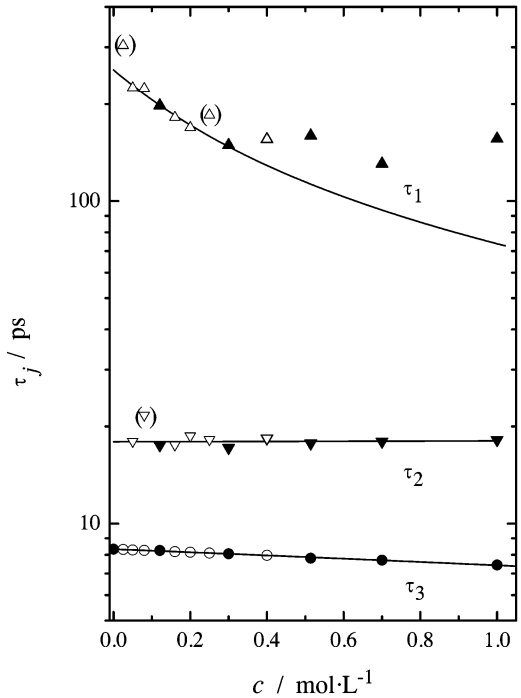

Figure 5. Measured relaxation times for processes 1−3 in $Na_2Su(aq)$ at 25 °C: obtained directly from wide-scan spectra (filled symbols) or interpolated from wide-scan spectra (τ_3) or obtained from $\nu \leq 20$ GHz spectra (τ_1, τ_2) with τ_3 fixed at the interpolated value (open symbols). The line through τ_1 at $c < 0.4$M was obtained with eq 8; bracketed points were not used.

is consistent with the relaxation time (τ_2) for process 2. Thus, τ_2 for $Na_2Su(aq)$ is virtually constant (17.9 ± 0.4ps) over the studied concentration range (Figure 5, Table 1), whereas τ_2 for $Na_2Ma(aq)$ increases from ∼15 to 18 ps (data not shown, cf. Table 1). Note that, at higher c, the τ_2 values for both salts, like the numbers of associated slow water molecules, are approximately equal.

The $Ma^{2-}(aq)$ ion is similar to $Ox^{2-}(aq)$ in that both appear to have a fragile hydration shell (one that decreases significantly with solute concentration). However, they differ with respect to the mobility of the water molecules within these shells (i.e.,

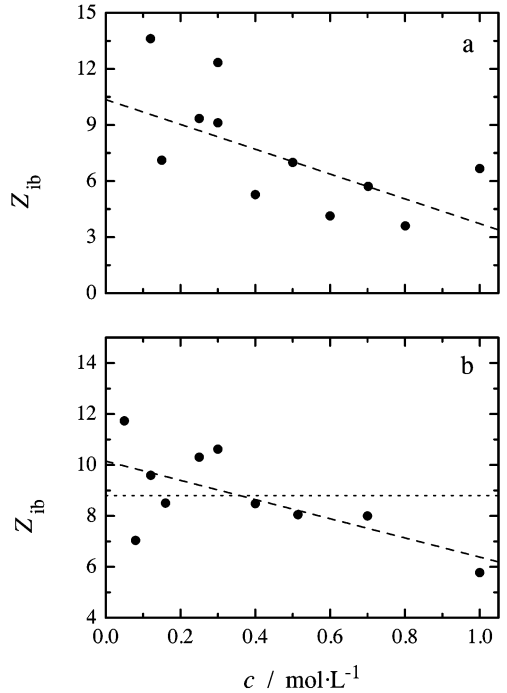

Figure 6. Effective solvation numbers, Z_{ib}, of (a) $Na_2Ma(aq)$ and (b) $Na_2Su(aq)$ at 25 °C, assuming slip boundary conditions for the kinetic depolarization effect.

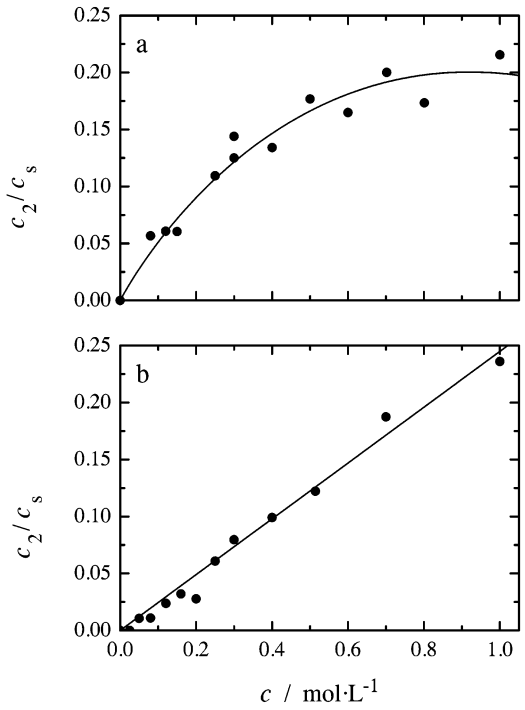

Figure 7. Fraction of slow water, c_2/c_s, for (a) $Na_2Ma(aq)$ and (b) $Na_2Su(aq)$ at 25 °C.

the rate of molecular rotation *and* exchange between their hydration shells and bulk water) relative to their tumbling rate in the electric field. The hydration-shell dynamics of Ox^{2-}(aq), which has irrotationally bound water molecules that are "frozen" on the DRS time scale, are clearly slower. Two size-related factors might be responsible for the greater mobility of water in the hydration shells of Ma^{2-}(aq) and Su^{2-}(aq). First, the decreasing separation of the carboxylate moieties ($Su^{2-} \rightarrow Ox^{2-}$) possibly enhances the cooperative $X^{2-}-H_2O$ interaction. Second, the lower tumbling rate of the larger X^{2-} ions might facilitate the separation of the slow water relaxation from the bulk process. By analogy with the present data for Ma^{2-}(aq) and Su^{2-}(aq), it might be anticipated that, at higher oxalate concentrations, it might be possible to identify an additional slow water process. This cannot be achieved with Na_2Ox because of its limited solubility (~0.25 M).[8]

TABLE 2: Ion-Pair Dipole Moments, μ_{IP}; Cavity Radii, r_{max}; and Resulting Parameters log K_A°, B_β, and C_β of Eq 6 for Some Ion-Pair Models of $NaMa^-$(aq) and $NaSu^-$(aq)[a]

structure		μ_{IP}	r_{max}	log K_A°	B_β	C_β
				$Na_2Ma(aq)$		
CIP	side-on	11.7	3.3	2.00 ± 0.10	-2.3 ± 0.3	0.83 ± 0.18
SIP	side-on	27.5	5.5	0.93 ± 0.05	-1.50 ± 0.15	0.44 ± 0.09
2SIP	side-on	44.5	6.9	0.48 ± 0.05	-1.42 ± 0.14	0.40 ± 0.08
				$Na_2Su(aq)$		
CIP	cis side-on	9.38	5.1	2.37 ± 0.13	-3.0 ± 0.4	1.2 ± 0.2
SIP	trans	19.9	6.5	1.40 ± 0.04	-2.33 ± 0.12	0.85 ± 0.07
	cis end-on	38.5	6.5	0.73 ± 0.03	-2.10 ± 0.10	0.74 ± 0.06
2SIP	trans	25.0	8.0	1.16 ± 0.03	-2.21 ± 0.11	0.79 ± 0.06
	cis end-on	43.7	8.0	0.62 ± 0.03	-2.08 ± 0.10	0.73 ± 0.05

[a] Units: μ_{IP} in D (1 D = 3.3356×10^{-30} C·m), r_{max} in 10^{-10} m, B_β in L·mol^{-1}, C_β in L$^{3/2}$·mol$^{-3/2}$.

4.3. Quantitative Description of Ion Pairing. As noted above, the very small amplitude, slowest process, centered on ~1 GHz (Figure 3), can be reasonably assigned to the existence of ion pairs. Unfortunately, as shown in detail below, the interpretation of this process is complicated by the internal flexibility of the anions. However, because the relaxation is of Debye type, it can be inferred that a single ion-pair species predominates.

The observed amplitudes (S_1) for this process were used to calculate the concentrations of the various possible ion-pair (IP) types, c_{IP}, using the procedure outlined in detail previously.[22,20] In essence, this involves using the Cavell[23] equation

$$c_{IP} = \frac{(2\epsilon + 1)}{\epsilon} \frac{k_B T \epsilon_0}{N_A} \frac{(1 - \alpha_{IP} f_{IP})^2}{\mu_{IP}^2} \times S_{IP} \qquad (5)$$

where k_B and N_A are the Boltzmann constant and Avogadro's number, respectively; α_{IP}, f_{IP}, and μ_{IP} are the polarizability, cavity-field factor, and dipole moment of the ion pair; and T is the (Kelvin) temperature. The polarizabilities of the various types of ion pairs were calculated as $\alpha_{IP} = \alpha_{IP}^0 + n'\alpha(H_2O)$, where n' is the number of H_2O molecules in the IP structure ($n' = 0$ for a contact ion pair, CIP; $n' = 1$ for a solvent-shared ion pair, SIP; $n' = 2$ for a double-solvent-separated ion pair, 2SIP). The values of $\alpha_{IP}^0/4\pi\epsilon_o = (8.69 \pm 0.04) \times 10^{-30}$ m^{-3} for $NaMa^-$ and $\alpha_{IP}^0/4\pi\epsilon_o = (10.49 \pm 0.13) \times 10^{-30}$ m^{-3} for $NaSu^-$ were obtained from refractive index measurements as described previously for $NaOx^-$;[8] see section 3. The value of $\alpha(H_2O)/4\pi\epsilon_o = 1.45 \times 10^{-30}$ m^3 was taken from the literature.[24] Because of the irregular shape of the relaxing species (the IPs), a spherical cavity and reaction field corresponding to their longest axis (cavity radius r_{max}) were assumed in eq 5.[23] The CIP dipole moments were obtained with MOPAC (PM3), whereas for the other species, μ_{IP} was calculated from $r(Na^+) = 98$ pm and $r(H_2O) = 142.5$ pm[24] and the X-ray data of Oskarsson et al.[25] for Ma^{2-} and of Fonseca et al.[26] for Su^{2-}. The quantities required for the evaluation of eq 5 are listed in Table 2 or are easily calculated using the relevant equations in Buchner et al.[20]

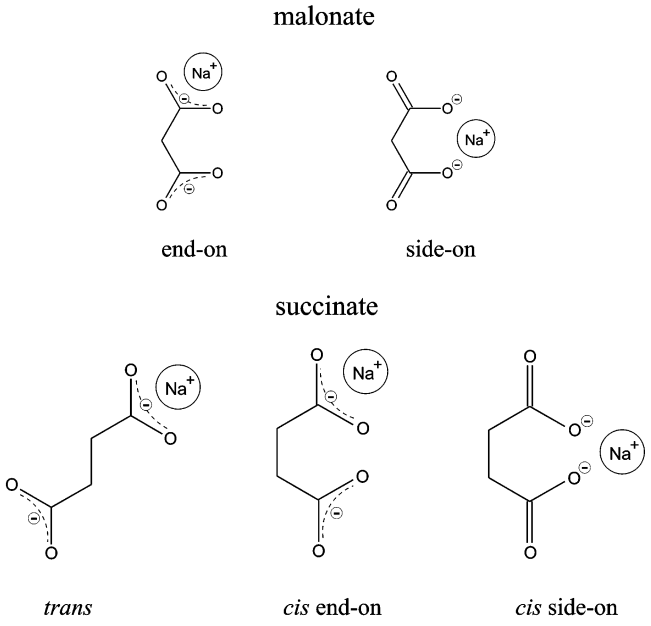

Figure 8. Possible CIP chelate structures for $NaMa^-$ and $NaSu^-$ (note that steric requirements allow only the end-on trans structure).

The concentrations of the various ion-pair types were then used to calculate the corresponding association constant, K_A, for the equilibrium

$$Na^+(aq) + X^{2-}(aq) \underset{k_{21}}{\overset{k_{12}}{\rightleftharpoons}} NaX^-(aq) \qquad (I)$$

where $NaX^-(aq)$ can be 2SIP, SIP, or CIP and k_{12} and k_{21} are the rate constants for the formation and dissociation, respectively, of the ion pair. To determine the standard (infinite dilution) association constant, K_A°, the values of K_A so obtained were then fitted for convenience to a Guggenheim-type function

$$\log K_A = \log K_A^\circ - \frac{2A_{DH}|z_+z_-|\sqrt{I}}{1+\sqrt{I}} + B_\beta I + C_\beta I^{3/2} \qquad (6)$$

where A_{DH} is the Debye−Hückel parameter for activity coefficients of electrolytes in water, B_β and C_β are empirical constants, and I is the ionic strength.[6] The K_A° values so determined for the various types of ion pair can then be plotted against the reciprocal of their calculated dipole moments. This provides a useful means of comparing estimated and experimental K_A° values and helps in choosing the most probable ion-pair structure.[27]

4.4. Possible Ion-Pair Structures. The determination of the likely ion-pair structures in the present systems is more complicated than in previous investigations,[8,27] because of the internal flexibility of Ma^{2-} and Su^{2-}. Thus, the possibilities of not only 2SIP, SIP, and CIP but also the various conformers and isomers must be considered. *Some* of the possibilities (using CIPs for simplicity of representation) are illustrated in Figure 8. In addition to the "chelates" shown, "monodentate" complexes are also possible but are likely to be less stable;[8] of course, there are the equivalent 2SIP and SIP possibilities.[28]

4.5. Sodium Malonate Solutions. For this electrolyte, the situation is relatively straightforward. MOPAC calculations suggest that the "side-on" structure is the most stable of the CIP possibilities. For the SIP and 2SIP species, the "end-on" and side-on chelate structures have similar dipole moments and thus cannot be distinguished by DRS. The values of log K_A obtained for sodium malonate solutions via eq 6 assuming an SIP are plotted as a function of I in Figure 9, curve 1. The data conform closely to the Guggenheim model (solid line), enabling reasonable estimation of log K_A°. The value thus obtained, log K_A°(SIP) = 0.92 ± 0.05, closely matches that of Daniele et al.,[29] log K_A° = 0.91, derived from glass electrode potentiometric data. This enables identification of the relaxing species as an end-on or side-on chelated SIP, because the alternative IP structures yield log K_A°(CIP) = 1.99 ± 0.10 and log K_A°(2SIP) = 0.48 ± 0.04.

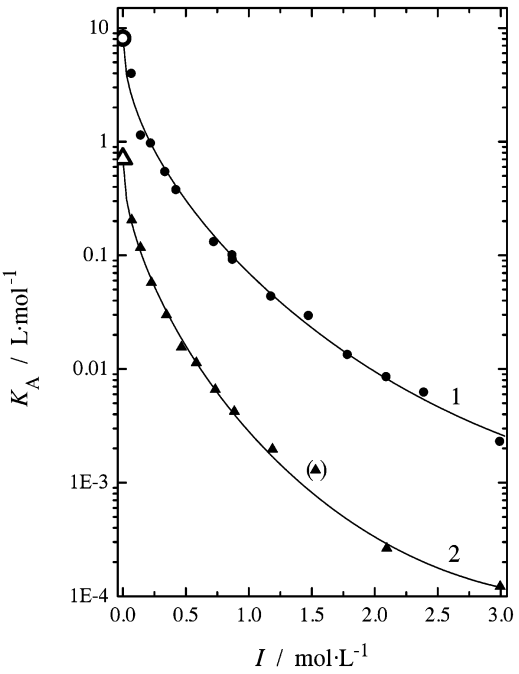

Figure 9. Association constants (K_A) for $NaMa^-$(aq) (●) and $NaSu^-$(aq) (▲, ×0.1 for representational clarity) as a function of ionic strength at 25 °C assuming SIP structures. The lines are Guggenheim-type fits to the data (eq 6, see text). Also included are the K_A° values of Daniele et al.[29] (open symbols).

As was found for Na_2Ox(aq)[8] and Na_2Su(aq) solutions (Figure 5), there is a significant decrease at low solute concentrations (c < 0.4 M) in the relaxation time of the ion pair, τ_1, for Na_2Ma(aq) (Table 1). This is indicative of a chemical kinetic contribution to the relaxation time of the ion pair. As shown previously,[8,30] if a single-step equilibrium for the formation of the ion pair is assumed, then the observable relaxation rate is given by

$$\tau_1^{-1} = (\tau_{IP}^{rot})^{-1} + (\tau_{ch})^{-1} \qquad (7)$$

where τ_{IP}^{rot} is the rotational correlation time and τ_{ch} is the kinetic ("chemical") relaxation time. The latter is given by

$$(\tau_{ch})^{-1} = k_{21} + 2k_{12}(3c - 2c_{IP}) \qquad (8)$$

A plot of τ_1^{-1} against I (not shown) is linear at c < 0.4 M, which indicates the formation of only one ion-pair type. The slope of this plot gives $k_{12} = (2.9 \pm 0.3) \times 10^9$ L·mol^{-1}·s^{-1}, which is 1/9 of the diffusion-controlled limit estimated from the limiting anion conductivity.[31] Combination of this value with K_A° yields $k_{21} = (3.4 \pm 0.5) \times 10^8$ s^{-1}, which corresponds to an ion-pair lifetime, $\tau_L = (\ln 2)/k_{21} = 2.0 \times 10^{-9}$ s, about 18 times larger than expected for diffusion-controlled decay.[30] The value of $\tau_{IP}^{rot} \approx 250$ ps roughly conforms with the expected rotational correlation time of an SIP.[8]

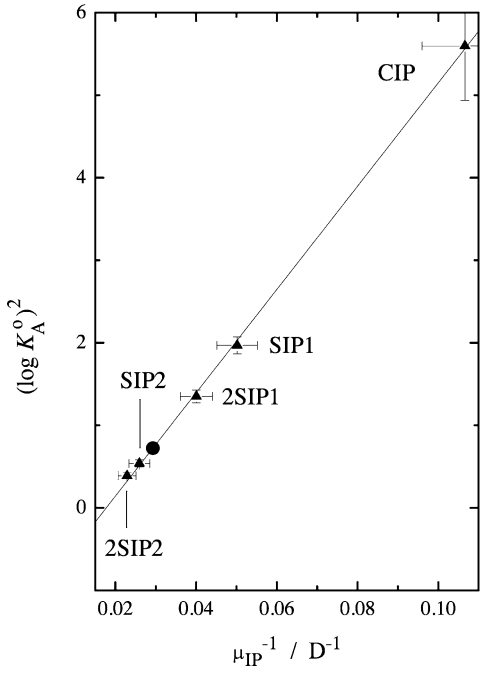

Figure 10. Values of $(\log K_A^\circ)^2$ obtained from S_1 with eq 6 for various ion-pair structures plotted against the reciprocal of the ion-pair dipole moment, μ_{IP}^{-1}. SIP1 and 2SIP1 represent the trans end-on structures and SIP2 and 2SIP2 the cis end-on structures. Values for cis side-on structures excluded for representational convenience (see text); value of Daniele et al.[29] (●) obtained from potentiometric measurements.

4.6. Sodium Succinate Solutions. As is apparent from Figures 1 and 2, the DRS spectra for $Na_2Su(aq)$ were qualitatively similar to those of $Na_2Ma(aq)$. However, their interpretation is more difficult because of the extra rotational freedom associated with the presence of the additional C−C bond in Su^{2-}. This increased flexibility results in widely varying estimates of the dipole moments of the possible ion pairs (Figure 8). Of the various CIP structures, MOPAC calculations indicate that the cis side-on structure is the most stable. For SIPs and 2SIPs, respectively, consideration of all chelated isomers (cf. Figure 8) gave dipole moment ranges of $20 \leq \mu_{SIP}/D \leq 39$ and $25 \leq \mu_{2SIP}/D \leq 44$, where the lower estimates refer to the trans and the higher to the cis end-on conformations (Table 2). This variation in μ_{IP} produces widely varying and overlapping estimates of K_A° (Figure 10). Note that the dipole moments of the cis side-on SIP and 2SIP structures, not included in Figure 10, are slightly smaller (K_A° larger) than the corresponding cis end-on values.

Despite these complications, the constancy of the IP relaxation time (a single Debye model adequately accounts for all of the features of the IP process) suggests that there is only one type of IP and that it has a well-defined conformation. On the basis of the chelate effect, it might be anticipated that a cis side-on conformation (Figure 8) would probably be the most stable structure. On the other hand, it is important to recognize that hydration effects are almost certainly critical and, therefore, the relative stabilities of the various conformers in *solution* could easily change for such weak complexes. The value of $\log K_A^\circ = 0.85$ derived from potentiometric data[29] corresponds most closely to that of a cis side-on SIP [with $k_{12} = (3.2 \pm 0.3) \times 10^9$ L·mol^{-1}·s^{-1} and $k_{21} = (6.0 \pm 0.4) \times 10^8$ s^{-1}]. However, because of the uncertainties, it is not possible to use Figure 10 to distinguish definitively between the side-on and end-on conformers or indeed between the SIP and 2SIP structures. If it is *assumed* [based on the good agreement between the potentiometric and DRS values for $\log K_A^\circ(NaMa^-)$ demonstrated above] that the $\log K_A^\circ(NaSu^-)$ value of Daniele et al.[29] is correct, a dipole moment of $\mu_{IP}(NaSu^-) = 34.2$ D is obtained. For an SIP structure, the experimental amplitudes, S_1, then yield the K_A values shown in Figure 9, which can be fitted with eq 6 with $\log K_A^\circ$ fixed to 0.85[29] and parameters $B_\beta = -2.13 \pm 0.05$ L·mol^{-1} and $C_\beta = 0.75 \pm 0.03$ L$^{3/2}$·mol$^{-3/2}$.

These findings must be viewed with caution, and it is emphasized that, in the absence of direct information about the actual conformation of the various ion-pair types in *solution*, it is not possible to use the present DRS data alone to unequivocally determine the IP structure for either $NaMa^-(aq)$ or $NaSu^-(aq)$. In this context, a high-quality molecular dynamics simulation would be particularly useful to resolve some of the uncertainties. As the ion pairs detected are solvent-separated, it is unlikely that either NMR or vibrational spectroscopy would be able to "see" these species. On the other hand, such studies might provide useful information on the conformation of the anions and on their interactions with water.

References and Notes

(1) Sloth, M.; Jørgensen, S.; Bilde, M.; Mikkelsen, K. V. *J. Phys. Chem. A* **2003**, *107*, 8623.
(2) Diem, K., Lentner, C., Eds. *Scientific Tables*, 7th ed.; Geigy Pharmaceuticals: Macclesfield, U.K., 1970.
(3) Metzler, D. E. *Biochemistry*; Academic Press: New York, 1977; p 526.
(4) Lever, G. *Light Metals* **1978**, 71.
(5) Königsberger, E.; May, P. M.; Hefter, G. T., manuscript in preparation.
(6) Robinson, R. A.; Stokes, R. H. *Electrolyte Solutions*, 2nd ed.; Butterworth: London, 1970.
(7) Zaytsev, I. D.; Asayev, G. G. *Properties of Aqueous Solutions of Electrolytes*; CRC Press: Boca Raton, FL, 1992.
(8) Buchner, R.; Samani, F.; May, P. M.; Sturm, P.; Hefter, G. T. *ChemPhysChem* **2003**, *4*, 373.
(9) May, P. M. In *Comprehensive Medicinal Chemistry*; Hansch, C., Sammes, P. G., Taylor, J. B., Eds.; Pergamon Press: Oxford, U.K., 1990; Vol. 2.
(10) Buchner, R.; Hefter, G. T.; May, P. M. *J. Phys. Chem. A* **1999**, *103*, 1.
(11) Barthel, J.; Bachhuber, K.; Buchner, R.; Hetzenauer, H.; Kleebauer, M. *Ber. Bunsen-Ges. Phys. Chem.* **1991**, *95*, 853.
(12) Barthel, J.; Buchner, R.; Eberspächer, P. N.; Münsterer, M.; Stauber, J.; Wurm, B. *J. Mol. Liq.* **1998**, *78*, 82.
(13) Born, M. *Optik*, 3rd ed. (reprint); Springer: Berlin, 1972.
(14) Pyper, N. C.; Pike, C. G.; Edwards, P. P. *Mol. Phys.* **1992**, *76*, 353.
(15) Buchner, R.; Barthel, J.; Stauber, J. *Chem. Phys. Lett.* **1999**, *306*, 57.
(16) Naganuma, H.; Kameda, Y.; Usuki, T.; Uemura, O. *J. Phys. Soc. Jpn. Suppl. A* **2001**, *70*, 356.
(17) Buchner, R.; Hölzl, C.; Stauber, J.; Barthel, J. *Phys. Chem. Chem. Phys.* **2002**, *4*, 2169.
(18) Baar, C.; Buchner, R.; Kunz, W. *J. Phys. Chem. B* **2001**, *105*, 2906.
(19) Fernandez, P.; Schrödle, S.; Buchner, R.; Kunz, W. *ChemPhysChem* **2003**, *4*, 1065.
(20) Buchner, R.; Capewell, S. G.; Hefter, G. T.; May, P. M. *J. Phys. Chem. B* **1999**, *103*, 1185.
(21) Buchner, R.; Chen, T.; Hefter, G. T. *J. Phys. Chem. B* **2004**, *108*, 2365.
(22) Barthel, J.; Hetzenauer, H.; Buchner, R. *Ber. Bunsen-Ges. Phys. Chem.* **1992**, *96*, 1424.
(23) Cavell, E. A. S.; Knight, P. C.; Sheikh, M. A. *J. Chem. Soc., Faraday Trans.* **1971**, *67*, 2225.
(24) Marcus, Y. *Ion Properties*; Marcel Dekker: New York, 1997.
(25) Oskarsson, Å. *Acta Crystallogr.* **1978**, *B34*, 1350.
(26) Fonseca, I.; Martınez-Carrera, S.; Garcıa-Blanco, S. *Acta Crystallogr.* **1986**, *C42*, 1123.
(27) Buchner, R.; Hefter, G. T. *J. Solution Chem.* **2002**, *31*, 521.
(28) The words chelate and monodentate are used for convenience to describe the geometry of the species. They do not imply anything about the nature of the bonding. This is especially true for the SIP and 2SIP species.
(29) Daniele, P. G.; DeRobertis, A.; Rigano, C. *J. Chem. Soc., Dalton Trans.* **1985**, 2353.
(30) Buchner, R.; Barthel, J. *J. Mol. Liq.* **1995**, *63*, 55.
(31) Apelblat, A.; Barthel, J. *Z. Naturforsch.* **1992**, *A47*, 493.